AN INVESTIGATION INTO THE USE OF TRANSIENT WAVE PACKETS FOR THE SIMULATION OF SPUDCAN IMPACTS WHEN GOING ON LOCATION

K.R. Drake*

Noble Denton marine services, DNV GL - Oil & Gas

**email address: kevin.drake@dnvgl.com*

ABSTRACT

Defining limiting conditions for jack-up units going on location requires risk assessments to be made of spudcan-seabed impacts that may arise during leg lowering. Recent progress in analysis methods has involved extensive use of time domain simulations with random waves and the development of simplified methods. This paper considers an alternative simplified method based upon transient wave packets that are tailored to produce synthesised extreme events that are representative of random conditions and that have prescribed probabilities of occurrence. The simulations are of short duration and provide direct evaluation of the expected concurrent rigid body motions associated with extreme spudcan velocity events in the freely floating condition. In the representative case considered, the largest vertical impacts are found to arise when the spudcan-seabed clearance is reduced by about 40% from the minimum clearance required to avoid impact. It is apparent that the analysis of isolated impacts with prescribed initial velocities, based on the freely floating condition, can provide a satisfactory prediction of impacts within the range of practical interest for the case studied. It is shown that the expected concurrent rigid body motions associated with extreme spudcan velocities in the freely floating condition can be obtained by multiplying the independent most probable maximum extreme (MPME) values by the corresponding correlation coefficients of the random process.

KEY WORDS: Cummins equation; jack-up; spudcan impact; transient wave packet; correlation coefficient.

INTRODUCTION

Recent progress in the analysis of limiting conditions for jack-up units going on location has involved the extensive use of time domain simulations with random waves. Tan et al. [1] carried out simulations in random waves with varying spudcan-seabed clearance and developed simplified methods suitable for routine analyses. One of the methods involves using a set of regular waves of different periods and heights selected to produce the same peak velocity response of the spudcan in the freely floating condition as the extreme response predicted using linear spectral methods. Such an approach involves consideration of a range of combinations of heave and pitch/roll motions.

An alternative approach is investigated in this paper using transient wave packets that have been tailored to produce impact events with a prescribed probability of occurrence. The possible advantages include not only the computational benefit of short duration simulations but also direct evaluation of the expected concurrent rigid body motions (e.g. heave and pitch) associated with extreme spudcan velocities. The paper is a follow-up to Drake and Zhang [2] and includes some restatement of formulation and model description.

THEORETICAL FORMULATION

Cummins [3] derived a linear time domain equation to represent the dynamics of a large floating marine structure in waves. An inviscid, incompressible fluid undergoing irrotational flow is assumed. The equation is referred to as the Cummins equation. Following the exposition and nomenclature of Chen et al. [4], it has the following form for a floating rigid body:

$$[\mathbf{M}+\mathbf{A}(\infty)]\ddot{\mathbf{x}}(t)+\int_0^t \mathbf{h}(t-\tau)\dot{\mathbf{x}}(\tau)d\tau+\mathbf{K}\mathbf{x}(t)=\mathbf{f}^{exc}(t) \qquad (1)$$

where, $\mathbf{x}$ is the vector of the rigid body degrees of freedom and a dot denotes time derivative; $\mathbf{M}$ is the mass matrix; $\mathbf{A}(\infty)$ is the constant positive-definite infinite-frequency added mass matrix; the kernel of the convolution term $\mathbf{h}(t)$ is the matrix of retardation functions and is linked to fluid memory effects; $\mathbf{K}$ is the

hydrostatic stiffness matrix; and $\mathbf{f}^{exc}(t)$ is the vector of wave excitation forces and moments that vary with time, t.

The retardation functions can be obtained by evaluating the following integral:

$$\mathbf{h}(t) = \frac{2}{\pi}\int_0^\infty \mathbf{B}(\omega)\cos(\omega t)\,d\omega \tag{2}$$

where $\mathbf{B}(\omega)$ is the positive definite matrix of hydrodynamic radiation damping coefficients at frequency ω.

Hydrodynamic coefficients can be readily obtained over a finite range of frequencies using three-dimensional panel codes. These are based on the use of boundary integral methods to solve the potential flow problem. Additional damping is required to account for viscous effects associated with pitch and roll motions.

We now consider the formulation of the transient wave packets and consider how they may be tailored to synthesise wave sequences that are especially relevant to the simulation of spudcan impacts. To do this we make use of the extensive research that has been undertaken to characterise the time history in the vicinity of a large peak within a stationary normal (or Gaussian) random process. This includes theoretical work by Lindgren [5] concerning the mathematical analysis of a stationary normal process in the vicinity of a local maximum and later work by Boccotti [6] specifically directed at investigating the statistical properties of wind waves. It has been shown that in the vicinity of a large local maximum that the expected time history of the random variable becomes increasingly deterministic and that it tends towards the autocorrelation function of the random process for increasingly large peaks. Tromans et al. [7] advocated the use of the autocorrelation function of wave surface elevation as the basis for the formulation of a transient design wave for fixed offshore jacket structures. The associated design methodology was referred to as NewWave.

In previous work, the author has proposed using the autocorrelation function of a vessel response parameter to represent the extreme time history of that parameter when the vessel responds linearly to unidirectional Gaussian random waves [8]. The autocorrelation function is easily found from the inverse Fourier transform of the appropriate response spectrum. Applying this approach to the case of a jack-up unit going on location, we take the spudcan vertical velocity in the freely floating condition as the parameter to be considered when deriving the transient wave packets to be used for the subsequent nonlinear assessment of spudcan-seabed impacts. The validity of this approach rests upon the hypothesis that wave groups causing extreme spudcan vertical velocity events in the freely floating condition are closely correlated with extreme seabed impact events that may arise during leg lowering.

Thus, the expected time history of spudcan vertical velocity in the vicinity of an extreme velocity event in the freely floating condition may be computed (in terms of spectral density) by scaling its autocorrelation function as follows:

$$\begin{aligned}\dot{\zeta}^*(\tau) &= \frac{\alpha}{\sigma_{\dot{\zeta}}^2}\int_0^\infty S_{\dot{\zeta}}(\omega)\cos(\omega\tau)\,d\omega \\ &\approx \frac{\alpha}{\sigma_{\dot{\zeta}}^2}\sum_{n=1}^{N} S_{\dot{\zeta}}(\omega_n)\cos(\omega_n\tau)\Delta\omega_n\end{aligned} \tag{3}$$

where $\dot{\zeta}^*$ is the expected vertical velocity of the spudcan, τ is the time relative to the extreme event, α is the extreme velocity, $\sigma_{\dot{\zeta}}$ is the standard deviation of the velocity and $S_{\dot{\zeta}}$ is the spectrum of the velocity.

The amplitudes and phases of the various wave components for the associated unidirectional incident transient wave packet that would cause this response are obtained by dividing the frequency components of the expected spudcan velocity time history by the corresponding values of the appropriate linear transfer

function. Thus, the wave elevation time history associated with the extreme vertical velocity event is obtained from the following summation:

$$\eta^*_{\dot{\zeta}}(\tau) = \frac{\alpha}{\sigma^2_{\dot{\zeta}}} \mathrm{Re}\left\{ \sum_{n=1}^{N} \frac{S_{\dot{\zeta}}(\omega_n)}{H_{\dot{\zeta}}(\omega_n)} \exp[i\omega_n \tau] \Delta\omega_n \right\}$$
$$= \frac{\alpha}{\sigma^2_{\dot{\zeta}}} \mathrm{Re}\left\{ \sum_{n=1}^{N} S_{\eta}(\omega_n) \overline{H_{\dot{\zeta}}}(\omega_n) \exp[i\omega_n \tau] \Delta\omega_n \right\} \qquad (4)$$

where, η^* is the expected free surface elevation time history at the origin of the wave coordinate system and the subscript denotes association with spudcan vertical velocity, S_η is the spectral density of wave surface elevation, $H_{\dot{\zeta}}$ is the linear transfer function for spudcan vertical velocity and the use of an overbar denotes the complex conjugate.

Once the wave elevation time history has been defined, it is a straightforward matter to compute the time history associated with any linearly related response parameter. Thus, the associated time history of the wave excitation load associated with rigid body displacement component ξ (e.g. heave or pitch) is given by

$$f^{exc*}_{\xi}(\tau) = \frac{\alpha}{\sigma^2_{\dot{\zeta}}} \mathrm{Re}\left\{ \sum_{n=1}^{N} S_{\eta}(\omega_n) \overline{H_{\dot{\zeta}}}(\omega_n) H_{f^{exc}_{\xi}}(\omega_n) \exp[i\omega_n \tau] \Delta\omega_n \right\} \qquad (5)$$

where $H_{f^{exc}_{\xi}}$ is the complex linear transfer function for the wave excitation load.

In this paper we use (5) to obtain the forcing on the right-hand side of the Cummins equation. All of the associated hydrodynamic coefficients and linear transfer functions are computed using frequency domain methods.

HYDRODYNAMIC LOADING FOR A REPRESENTATIVE HULL

Figure 1 shows the panel mesh for a hydrodynamic model of a representative hull as presented in [2]. The main simplification compared to a more realistic model of a jack-up rig is the omission of leg wells. Hydrodynamic coefficients were computed at 30 different frequencies over the range 0.105 to 1.795 rad/s (0.0167 to 0.2857 Hz) using AQWA [9].

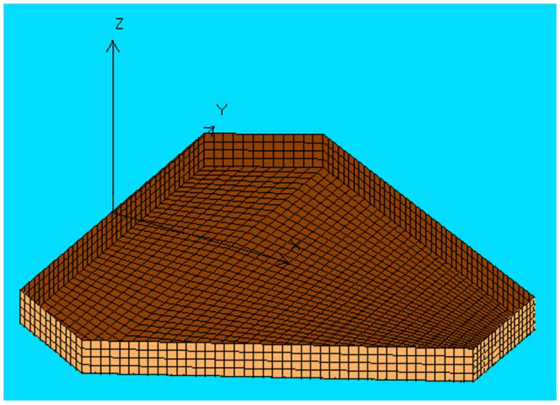

Figure 1 Hydrodynamics panel model (AQWA plot)

Spline interpolation was used to provide values of radiation damping at 151 frequencies with uniform spacing from zero up to 1.795 rad/s. The retardation functions were computed at time intervals of 0.02s using the trapezoidal rule. The convolutions in (1) can become very time consuming for long simulations with random waves. Substantial improvements in computational efficiency can be obtained by approximating the

convolutions with a state-space model (e.g.[4]). However, such an approach is not necessary for the short duration transient wave packets considered in this paper.

SIMPLIFIED STRUCTURAL MODEL

Figure 2 provides an illustration of a simplified two-dimensional linear elastic structural model that is considered sufficient for the purposes of this investigation.

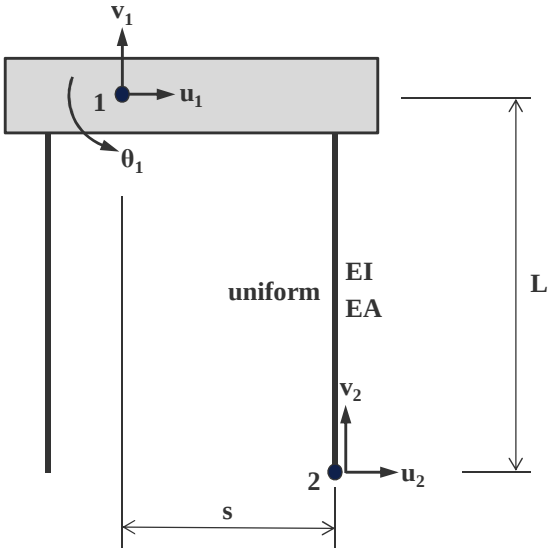

Figure 2 Schematic of simplified 2-D linear elastic structural model

A rigid hull is connected to a single leg which has cross-sectional area A and second moment of area I. The leg material has a modulus of elasticity E. The horizontal offset of the leg from the hull centre of gravity is s and the length of the leg is L. The model has five degrees-of-freedom (5DOF): surge, heave and pitch of the hull (u_1, v_1, θ_1) and horizontal and vertical translation of the bottom of the leg (u_2, v_2). The hull has hydrostatic restoring stiffness k_{v1} in heave and $k_{\theta 1}$ in pitch. Vertical and horizontal elastic springs with stiffness k_{v2} and k_{h2} are provided at the bottom of the leg and are active only when contact is made with the seabed. It may be shown that the 5DOF model has the following stiffness matrix:

$$\mathbf{K} = \begin{bmatrix} \frac{3EI}{L^3} & 0 & \frac{3EI}{L^2} & -\frac{3EI}{L^3} & 0 \\ 0 & \left(\frac{EA}{L}+k_{v1}\right) & \frac{EAs}{L} & 0 & -\frac{EA}{L} \\ \frac{3EI}{L^2} & \frac{EAs}{L} & \left(\frac{3EI}{L}+\frac{EAs^2}{L}+k_{\theta 1}\right) & -\frac{3EI}{L^2} & -\frac{EAs}{L} \\ -\frac{3EI}{L^3} & 0 & -\frac{3EI}{L^2} & \left(\frac{3EI}{L^3}+k_{h2}\right) & 0 \\ 0 & -\frac{EA}{L} & -\frac{EAs}{L} & 0 & \left(\frac{EA}{L}+k_{v2}\right) \end{bmatrix} \quad (6)$$

A computer program has been written in Fortran 90 in order to apply the Cummins equation to the analysis of the representative rig model. The constant acceleration method, as described by Clough and Penzien [10], has been implemented and extended to include the convolutions associated with the retardation functions.

IMPACTS IN WAVE GROUPS AND THE ROLE OF SEABED CLEARANCE

Here we consider a representative rig in head seas described by a Pierson-Moskowitz wave spectrum. The significant waveheight is 2m and the zero-crossing period is 7s (peak period is 9.86s). Details of the model are given in [2] and restated in Table 1. Only on-diagonal high-frequency asymptotes for added mass coefficients and on-diagonal retardation functions for heave and pitch are incorporated in the model; hydrodynamic effects in surge and coupling between the degrees of freedom are considered negligible. Additional pitch damping, equivalent to 5% of critical damping in the freely floating condition, is added to account for viscous effects. The chosen probability of occurrence of the extreme vertical velocity event is associated with the most probable maximum extreme (MPME) in 1000 peaks of a linear narrow band Gaussian random process, thereby giving a factor of 3.72 to be applied to the standard deviation of vertical velocity (i.e. $\sqrt{2\ln 1000}$).

Table 1 Model parameters

Hull length (m)	70.36
Hull width (m)	76.00
Hull depth (m)	9.40
Hull draught (m)	6.00
Hull waterplane area (m^2)	3,620
Hull second moment of waterplane area (m^4)	1.22 x 10^6
Hull and leg dry mass (tonnes)	22,265
Longitudinal leg spacing (m)	45.72
Transverse leg spacing (m)	47.55
Leg cross-sectional area (m^2)	0.537
Leg second moment of area (m^4)	15.373
Leg length, L (m)	70.00
Leg offset, s (m)	30.48
Radius of gyration for hull and legs (m)	37.69

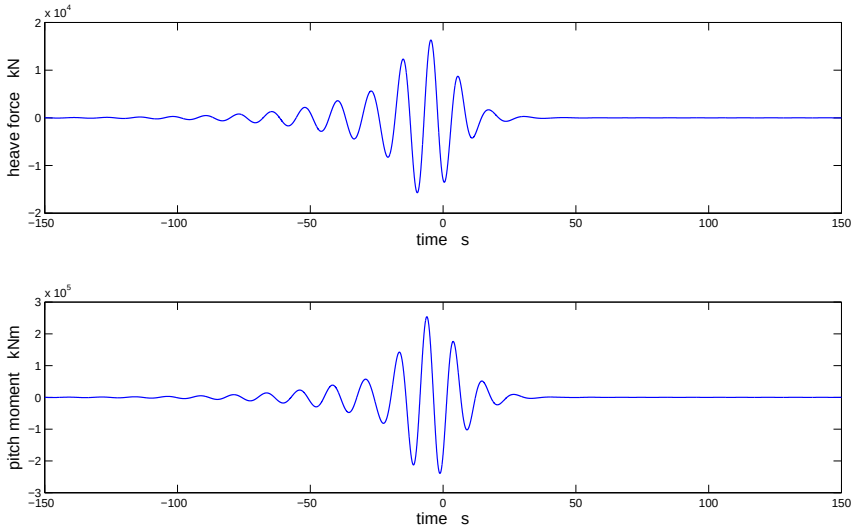

Figure 3 Wave excitation load time histories associated with spudcan velocity extreme event

Figure 3 shows the time histories of heave force and pitch moment that were computed using (5) and used as the wave excitation in the Cummins equation. Figure 4 shows the corresponding time histories of spudcan (bottom of leg) vertical velocity and vertical displacement in the freely floating condition. The time histories have been computed using two different methods: the blue solid line shows the values computed using the Cummins equation with the excitation time histories given in Figure 3; the red dashed line shows the values computed using (3) and frequency domain methods. The two sets of computed results are virtually indistinguishable, as would be expected for linear responses in the freely floating condition, and provide assurance that the Cummins equation has been implemented correctly within our computer program. Of

course, the sole purpose of using the Cummins equation in this paper is to represent jack-up hull-in-water hydrodynamics in the time domain in order that nonlinear simulation of seabed impacts can be undertaken.

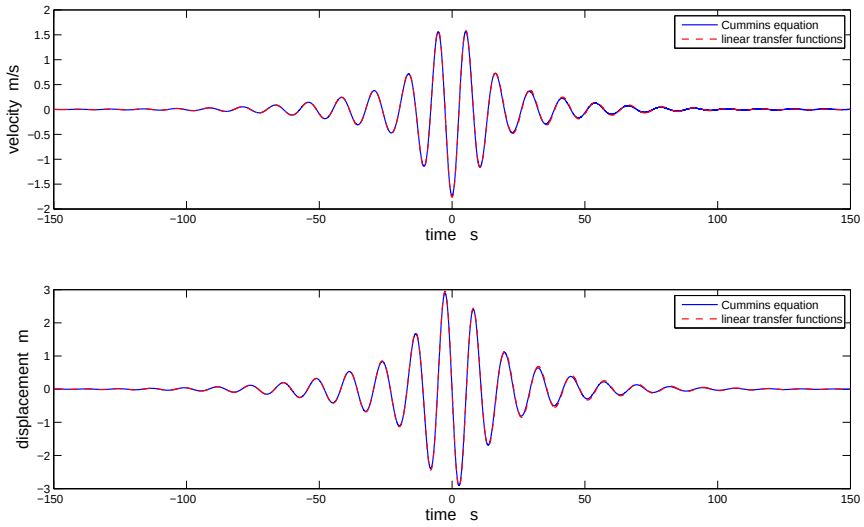

Figure 4 Spudcan vertical velocity and displacement time histories in the freely floating condition

The peak downward displacement of the spudcan in Figure 4 is 2.91m indicating the clearance required to avoid seabed impacts with this transient wave packet. Figure 5 shows the spudcan displacement time history for the case of 2m seabed clearance in the still water condition. As in [2], the values for seabed spring stiffness have been set equal to one quarter of the axial stiffness of the leg. The horizontal gridline at -2m represents the seabed datum. Three impacts (i.e. crossings at -2m) can be seen. The first impact causes a small reduction in the positive peak prior to the second impact, when compared with the magnitude of the corresponding positive peak in Figure 4 for the freely floating condition.

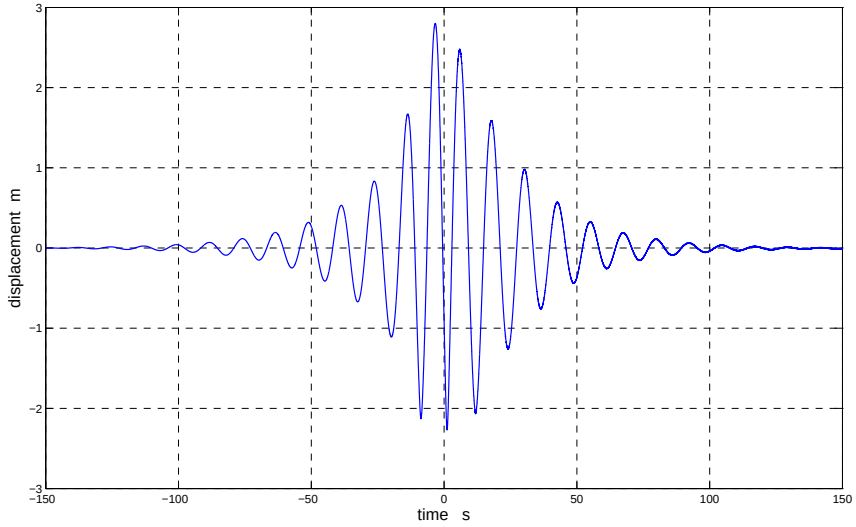

Figure 5 Spudcan vertical displacement time history with 2m seabed clearance

Figure 6 shows the spudcan displacement time history for the case of 1m seabed clearance in the still water condition. The horizontal gridline at -1m represents the seabed datum. There are four impacts (i.e. crossings at 1m). A significant reduction in the magnitude of the positive peaks can be seen after the second and third impacts when compared with the positive peaks after the first and second impacts in Figure 5.

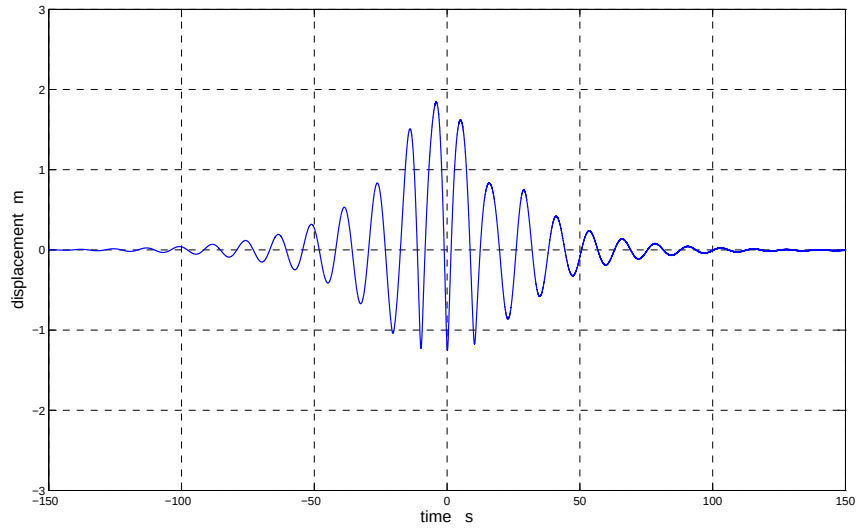

Figure 6 Spudcan vertical displacement time history with 1m seabed clearance

Figure 7 shows the largest seabed impact vertical displacements in transient wave packets obtained over a range of seabed clearance (0m to 2.75m in 0.25m increments, plus minimum clearance to avoid impact). The associated vertical impact forces are linearly proportional to displacement in the idealised case considered here of a linear elastic seabed; 0.3m seabed displacement corresponds to an impact force of 121MN (12,317 tonnes). We observe that as the clearance is reduced from the minimum clearance to avoid impact, there is a continual increase in the magnitude of the vertical impacts until the clearance is reduced by around 40%.

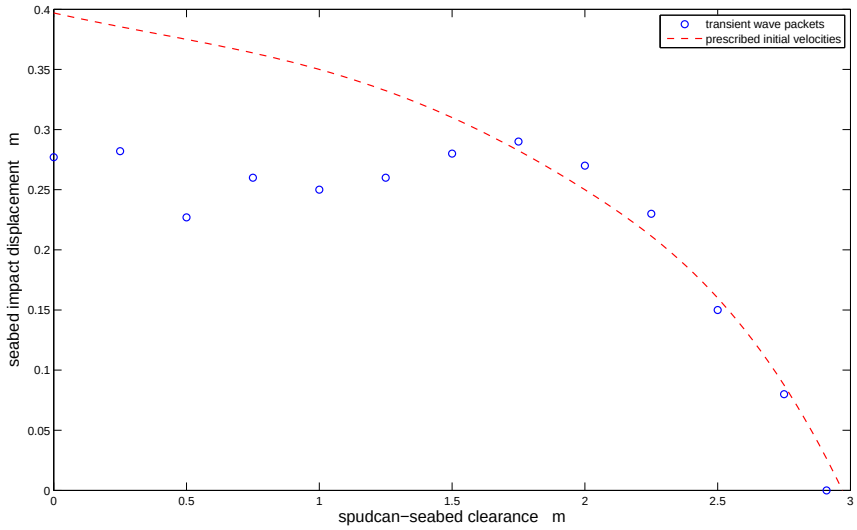

Figure 7 Comparison of seabed impacts due to transient wave packets and prescribed initial velocities

ISOLATED IMPACTS DUE TO PRESCRIBED INITIAL VELOCITIES WITH SEABED CLEARANCE

To make comparisons with established practices (as discussed in [2]), consideration has been given to isolated impacts in the absence of waves, using prescribed initial heave and pitch velocities associated with the extreme spudcan velocity event for a transient wave packet in the freely floating condition, as presented in Figure 4. The retardation functions and viscous damping were set to zero for the purposes of consistency with the barstool structural models often used for spudcan impact studies. The seabed clearance was increased in 0.25m increments until the minimum clearance to avoid impact was reached. A monotonic trend of impact displacement reducing with increasing clearance was obtained as shown by the smooth red-dashed line in Figure 7.

In the case that has been considered, we observe that the isolated impacts with prescribed initial velocities provide a very satisfactory proxy model for the prediction of impact displacements (and forces) when the seabed clearance is greater than or equal to 60% of the minimum clearance to avoid impact in the freely floating condition. The proxy model is observed to be conservative for smaller values of seabed clearance, but perhaps not excessively so for some practical situations.

The simulation of isolated impacts with prescribed initial velocities, as described here, neglects the following: the influence of earlier impacts on the motion of the jack-up unit; wave excitation loads; wave radiation due to jack-up motion (i.e. retardation functions); viscous damping in pitch. In terms of the simulated impacts, it is evident that the combination of these effects must be small over the range where satisfactory agreement is obtained with the more comprehensive simulations in transient wave packets.

CORRELATION COEFFICIENTS FOR RIGID BODY COMPONENTS OF IMPACT VELOCITIES

We now consider more closely the rigid body velocity components associated with an extreme spudcan velocity event in order to relate the concurrent velocities with their independent most probable maximum extremes (MPME). Following the method given in (5), the associated time history of the rigid body velocity component $\dot{\xi}$ (e.g. heave or pitch) is given by

$$\dot{\xi}^*_{\dot{\zeta}}(\tau) = \frac{\alpha}{\sigma^2_{\dot{\zeta}}} \mathrm{Re}\left\{ \sum_{n=1}^{N} S_\eta(\omega_n) \overline{H_{\dot{\zeta}}}(\omega_n) H_{\dot{\xi}}(\omega_n) \exp[i\omega_n \tau] \Delta\omega_n \right\} \tag{7}$$

where $H_{\dot{\xi}}$ is the complex linear transfer function between wave elevation and the rigid body velocity.

Thus, the rigid body velocity component at the time of the extreme event is given by

$$\dot{\xi}^*_{\dot{\zeta}}\Big|_{\tau=0} = \frac{\alpha}{\sigma^2_{\dot{\zeta}}} \mathrm{Re}\left\{ \sum_{n=1}^{N} S_\eta(\omega_n) \overline{H_{\dot{\zeta}}}(\omega_n) H_{\dot{\xi}}(\omega_n) \Delta\omega_n \right\} \tag{8}$$

Normalising the concurrent velocity with respect to its MPME value, β, we obtain

$$\frac{\dot{\xi}^*_{\dot{\zeta}}\Big|_{\tau=0}}{\beta} = \frac{\mathrm{Re}\left\{ \sum_{n=1}^{N} S_\eta(\omega_n) \overline{H_{\dot{\zeta}}}(\omega_n) H_{\dot{\xi}}(\omega_n) \Delta\omega_n \right\}}{\sigma_{\dot{\zeta}}\, \sigma_{\dot{\xi}}} = \rho_{\dot{\zeta}\dot{\xi}} \tag{9}$$

where $\rho_{\dot{\zeta}\dot{\xi}}$ is the correlation coefficient between the two random variables.

It is noted that the formulation differs from the phase cofactors methodology for joint seakeeping response processes as described by Hutchison [11] and originally proposed in 1978. Within the realm of offshore structures engineering, that methodology has found use in the assessment of transportation loads [12]. The difference arises in the time history used for the extreme event. In the phase cofactors formulation, all the amplitudes of the frequency components that might be used in a random simulation are put into phase (i.e. component amplitudes proportional to the square root of the spectral density). This differs from the expected time history in (3) where the amplitudes that are brought into phase are proportional to the spectral density of the random process. This is associated with large peaks being more likely to be formed by the most energetic components. The matter of concurrent responses is considered further in the Appendix wherein a derivation is given for the time dependent conditional probability density function of one jointly distributed random variable when another attains a peak value.

Table 2 presents the MPME velocities and correlation coefficients for the representative jack-up unit in four seastates defined by the Pierson-Moskowitz wave spectrum. The correlation coefficients have been

computed using (9). The concurrent heave and pitch velocities associated with the MPME spudcan vertical velocity are obtained by multiplying the MPME heave and pitch velocities by the corresponding correlation coefficients. The concurrent pitch velocities (rad/s) are multiplied by the leg offset of 30.48m before being added to the concurrent heave velocities to produce the values presented in the rightmost column. The consistency of the methodology is confirmed by the combined concurrent velocities being exactly equal to the MPME spudcan vertical velocities.

Table 2 MPME velocities and correlation coefficients

H_s m	T_2 s	T_0 s	MPME spudcan vertical velocity m/s	MPME pitch velocity rad/s	MPME heave velocity m/s	spudcan & pitch velocities correlation coefficient	spudcan & heave velocities correlation coefficient	Combined concurrent velocities m/s
2.0	8.0	11.26	-2.1303	-0.0472	-0.8411	0.9627	0.8865	-2.1303
2.0	7.0	9.86	-1.7642	-0.0363	-0.7767	0.9559	0.9080	-1.7642
2.0	6.0	8.45	-1.2001	-0.0210	-0.6288	0.9465	0.9444	-1.2001
2.0	5.0	7.04	-0.6444	-0.0093	-0.3819	0.9578	0.9771	-0.6444

As might be expected, there is a very high correlation between pitch velocities and spudcan vertical velocities over the range of seastates considered. Furthermore, the computed correlation coefficients lend support to the simplified practice of using the MPME pitch velocity in conjunction with sufficient heave velocity to match the MPME spudcan vertical velocity, when analysing isolated impacts with prescribed initial velocities.

CONCLUSIONS

An alternative simplified method has been implemented involving the use of tailored transient wave packets to synthesise short duration extreme spudcan velocity events that are representative of random conditions and that have prescribed probabilities of occurrence. In the representative case considered, the largest vertical impacts are found to arise when the spudcan-seabed clearance is reduced by about 40% from the minimum clearance required to avoid impact. It is also evident in the case studied that the analysis of isolated impacts with prescribed initial velocities, based on the freely floating condition in waves, can provide a satisfactory prediction of the largest impacts when the seabed clearance is close to half the minimum clearance required to avoid impact. Further work is recommended to consider a wider range of model properties than studied here, including leg dynamics and nonlinear hysteretic behaviour of the seabed, and to compare the impacts obtained with those predicted in regular and random waves.

It has been shown that the expected concurrent rigid body velocity components associated with extreme spudcan velocity events in the freely floating condition can be obtained by multiplying the independent MPME values by the corresponding correlation coefficients of the random process. This finding can be derived from the time dependent conditional probability density function of a jointly distributed random variable when another attains a peak value, as shown in the Appendix. The finding differs from the phase cofactors approach given by Hutchison [11].

ACKNOWLEDGEMENT

The author is grateful to Dr Peter Tromans of Ocean Wave Engineering Ltd for the consideration given to the author's derivation of conditional probability density functions for concurrent responses.

REFERENCES
[1] Tan, P., Chen, X., Yu, X., Perry, M., Mu, H., Chang, T., Wong, M. and Chen, D. Jackup going on location analysis. International Conference: The Jack-up Platform. Design, Construction & Operation. City, University of London, UK. September, 2015.
[2] Drake, K.R. and Zhang, Y. On the role of jack-up hull-in-water radiation impedance during spudcan impacts with the seabed. International Conference: The Jack-up Platform. Design, Construction & Operation. City, University of London, UK. September, 2015.
[3] Cummins, W.E. The impulse response function and ship motions. Hydromechanics Laboratory Research and Development Report. David Taylor Model Basin, 1962, Report 1661.
[4] Chen, M., Eatock Taylor, R., Choo, Y.S. Time domain modelling of a dynamic impact oscillator under wave excitations. Ocean Engineering, 2014, 76, 40-51.
[5] Lindgren, G. Some properties of a normal process near a local maximum. Ann Math Stat 1970; 41(6):1870-83.
[6] Bocotti, P. Some new results on statistical properties of wind waves. Applied Ocean Research 1983; 5(3): 134-40.
[7] Tromans, P.S., Anaturk, A.R., Hagemeijer, P. A new model for the kinematics of large ocean waves – application as a design wave. Proceedings of the First International Offshore and Polar Engineering Conference (ISOPE), Edinburgh, UK, 1991, vol.3, 64-71.
[8] Drake, K.R. Wave profile characterisation of green water loading events from model test data. Applied Ocean Research, 2001, 23, 187-193.
[9] Aqwa User's Manual, ANSYS Aqwa, Release 15.0, November 2013.
[10] Clough, R.W. and Penzien, J. Dynamics of Structures. Second Edition. McGraw-Hill, 1993.
[11] Hutchison, B.L. Joint seakeeping response processes for determining structural loads. Transactions of the Society of Naval Architects and Marine Engineers, 2002.
[12] Sircar, S., Austin, J.D. and Piermattei, E.J. Seakeeping Analysis of Self-Floating Steel Towers. OTC 5282, 18th Annual Offshore Technology Conference, Houston, Texas, 5-6 May, 1986.
[13] Price, W.G. and Bishop, R.E.D. Probabilistic theory of ship dynamics. Chapman & Hall, September 1974. ISBN-10: 0412124300.

APPENDIX – DERIVATION OF CONDITIONAL PROBABILITY DENSITY FUNCTIONS FOR CONCURRENT RESPONSES

The time histories for two jointly distributed Gaussian random variables with zero mean are shown in Figure 8. The random variable η attains a peak at time t_1. Tromans et al. [7] have shown how the conditional probability density function may be derived for η at time $t_1+\tau$. Here we follow their exposition and extend it to derive the conditional probability density function for ξ at time $t_1+\tau$.

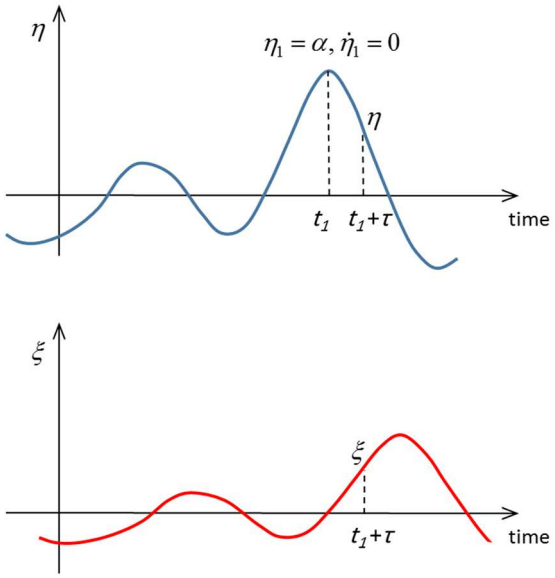

Figure 8 Time histories of a joint normal process when one random variable attains a peak value

The joint probability density function for three Gaussian random variables is readily obtained using standard formulation (e.g. [13]). Considering the case in Figure 8, the following expression for the joint probability density function may be obtained after some manipulation:

$$p(\xi,\ \eta_1=\alpha,\ \dot{\eta}_1=0)=B\exp\left[-\frac{\sigma^2\xi^2+\nu^2\left(1-\dot{\gamma}^2\right)\alpha^2-2\nu\sigma\gamma\alpha\xi}{2\nu^2\sigma^2\left(1-\gamma^2-\dot{\gamma}^2\right)}\right] \qquad \text{(A1)}$$

in which $B=\dfrac{1}{(2\pi)^{\frac{3}{2}}\nu\lambda\sigma^2\left(1-\gamma^2-\dot{\gamma}^2\right)^{\frac{1}{2}}}$ and

the variances and covariances are given by $\overline{\xi^2}=\nu^2$, $\overline{\eta_1^2}=\sigma^2$, $\overline{\dot{\eta}_1^2}=\lambda^2\sigma^2$, $\overline{\xi\eta_1}=\gamma\sigma\nu$, $\overline{\xi\dot{\eta}_1}=-\dot{\gamma}\lambda\sigma\nu$ where the overbar denotes time averaging. It should be noted at this point that there are some minor differences arising in the notation when compared with [7] and, of course, that the normalised cross-correlation functions γ and $\dot{\gamma}$ are functions of the time separation τ.

As in [7] the probability density function associated with the peak event is given by

$$p\left(\eta_1=\alpha\middle|\,\dot{\eta}_1=0\right)p(\dot{\eta}_1=0)=C\exp\left[-\frac{\alpha^2}{2\sigma^2}\right] \qquad \text{(A2)}$$

in which $C=\dfrac{1}{2\pi\sigma^2\lambda}$

Thus, the conditional probability density function for ξ when η has attained a peak value is obtained by dividing (A1) by (A2) and expressing as

$$p\left(\xi\middle|\,\eta_1=\alpha,\dot{\eta}_1=0\right)=\frac{1}{(2\pi)^{\frac{1}{2}}\sigma_2}\exp\left[-\frac{(\xi-m)^2}{2\sigma_2^2}\right] \qquad \text{(A3)}$$

where $\sigma_2=\nu\left(1-\gamma^2-\dot{\gamma}^2\right)^{\frac{1}{2}}$ and $m=\dfrac{\alpha\nu\gamma}{\sigma}$.

For a given separation in time, τ, we see that the conditional probability density function in (A3) is Gaussian with mean m and standard deviation σ_2. We note that α/σ is the ratio of MPME to standard deviation for the extreme peak event and ν is the standard deviation of ξ. Thus, the expected time history for ξ is the product of its MPME ($\alpha\nu/\sigma$) and the normalised cross-correlation function γ. At the instant of the peak event, when $\tau=0$, the value of the normalised cross-correlation function is equal to the correlation coefficient between the two random variables.

In the case of highly correlated random variables when $\tau\to 0$ then $\gamma\to 1$, $\dot{\gamma}\to 0$ and so $\sigma_2\to 0$. As in [7], we also note that m increases for larger peaks whilst σ_2 remains constant. The jointly distributed random variable ξ then becomes increasingly deterministic within the vicinity of the extreme peak event for η. This supports the emphasis that has been given to the expected concurrent values in the main text of the paper.